A V^{2+} ion in GaAs studied by thermally detected EPR

1992 J. Phys.: Condens. Matter 4 4565

(http://iopscience.iop.org/0953-8984/4/18/022)

J. Phys.: Condens. Matter 4 (1992) 4565–4582. Printed in the UK

A V^{2+} ion in GaAs studied by thermally detected EPR

A-M Vasson†§, A F Labadz‡¶, N Tebbal†§, A Vasson†§, A Gavaix†§ and C A Bates‡

† LPMC, Physique 4, Université Blaise Pascal Clermont-Ferrand II, 63177 Aubière-Cédex, France

‡ Physics Department, The University, Nottingham NG7 2RD, UK

Received 23 December 1991

Abstract. New thermally detected electron paramagnetic resonance (TD-EPR) experiments at 35 GHz, including photoinduced effects, are described. The resonances are attributed to a V^{2+}(II) centre with a $^4T_1$ ground state as before. In order to attempt to identify the nature of the centre, a trigonal model is presented which supposes that the V^{2+} ion is part of a complex in which one of the neighbouring As ions is replaced by a defect. It is shown that the TD-EPR results are consistent with such a model but this does not prove by itself that the V^{2+}(II) ion is part of a complex. Other experimental results obtained by other techniques are also discussed and related to the TD-EPR data obtained here. After consideration of all the available data, the most probable conclusion is that V^{2+}(II) is part of a complex.

1. Introduction

Vanadium in GaAs has been studied extensively since it was realised that vanadium doping can lead to thermally stable semi-insulating materials. The earlier studies have been reviewed by Clerjaud (1985), but subsequently numerous further publications have appeared concerning chiefly the electrical and optical properties of the system and the microscopic nature of the vanadium defects. For example, Bremond *et al* (1989) have located 'unambiguously' the V^{3+}/V^{2+} isolated single acceptor level of vanadium at $E_c - 0.14$ eV and also found that it is the only vanadium-related level lying within the band gap of GaAs, which is in agreement with many previous publications. (The term 'isolated' is used to denote that the vanadium ion is not associated or complexed with any other defect.) Also, Ko *et al* (1989) have shown that vanadium plays an important but direct role in the creation of the high resistivity of the GaAs:V samples as it 'getters' shallow donor impurities by reducing the value of their effective concentration below that of the shallow acceptors also present in the samples. Compensation occurs via the mid-gap EL2 donor level.

Another problem that has given rise to many studies concerns the nature of the ground state of the isolated V^{2+} ion. Does it have a high-spin $^4T_1$ ground state (in agreement with Hund's rule) or is the crystal field large enough so that the ^2E state lies lowest (as predicted theoretically by Katayama-Yoshida and Zunger (1986) and

§ Unité de Recherche Associé au CNRS 796.

¶ Now at: Manchester Computing Centre, University of Manchester, Oxford Road, Manchester M13 9PL, UK.

0953-8984/92/184565+18$04.50

Caldas *et al* (1986))? To attempt to answer this question it is necessary to examine the experimental evidence, together with suitable theoretical models.

From electric deep-level optical spectroscopy (DLOS) experiments, Bremond *et al* (1989) observed that the photoionization cross-section spectrum of the $E_c - 0.14$ eV level is very similar to the well known optical absorption (OA) spectrum (e.g., Clerjaud *et al* 1985, Hennel *et al* 1987, Ulrici *et al* 1985) with the peak of the main band around 1.0 eV. This confirms the first identification of this OA signal by Clerjaud *et al* (1985) as resulting from internal transitions of the isolated V^{2+} ion. This band and other related signals have been interpreted with either a $^4T_1$ or a ^2E ground state for the V^{2+} ion depending upon the authors. However, guided by the theoretical work cited above, it appears that a majority of authors favour ^2E as the ground state although the arguments for this choice are often unclear, as we discuss later.

In a comprehensive study of phonon scattering from thermal-conductivity experiments of 3d impurity ions in III–V semiconductors in the University of Nottingham laboratories, Challis and co-workers have concluded that E states scatter phonons significantly less strongly than do T_1 states. In particular, Sahraoui-Tahar *et al* (1989) have found that strong scattering of the phonons occurs for GaP:V but that in GaAs:V the scattering is much weaker (Butler *et al* 1989). They thus deduced that the ground state of the isolated V^{2+} ion in GaAs is ^2E but that in GaP the V^{2+} ground state is $^4T_1$.

Much information concerning the ground state of impurity ions in III–V semiconductors has usually been obtained from electron paramagnetic experiments (RPE) as summarized, for example, by Clerjaud (1985). Unfortunately, in vanadium-doped GaAs, conventional EPR only gives a signal from the V^{3+} ion which has an A_2 ground state (Kaufmann *et al* 1982). No resonance has been observed which can be attributed to the V^{2+} ion. However, optically detected magnetic resonance (ODMR) experiments at 24 GHz undertaken by Görger *et al* (1988) have shown the presence of a line with $g = 2.07$ in n-type GaAs:V samples. They interpret this resonance in terms of a V^{2+} centre (we shall discuss this result later). Nevertheless, it appears that the corresponding magnetic circular dichroism (MCD) is from a centre different from that responsible for the OA and DLOS spectra. It cannot then be due to the isolated V^{2+} ion. (The V^{3+} ion has also been detected in GaAs by these authors using ODMR.)

In a comprehensive study using thermally detected EPR (TD-EPR) between 8.0 and 12.4 GHz, on vanadium-doped GaAs samples, many intense resonance lines have been found. The first results were reported in Vasson *et al* (1984). Further data were given in Ulrici *et al* (1987) and En-Naqadi *et al* (1988). It was proposed there that the centre responsible for these spectra was V^{2+}, which was labelled as V^{2+}(II) in order to indicate that it was not expected to be the isolated V_{Ga}^{2+} ion. The same centre has also been observed in GaAs by acoustic paramagnetic resonance (APR) experiments by Rampton *et al* (1986) and by acoustically detected EPR (AD-EPR) by Vasson *et al* (1986). It must also be noted that Butler *et al* (1989) have assigned the two strong phonon resonances seen at low frequencies to this V^{2+}(II) centre in GaAs:V.

Recent TD-EPR experiments at 35 GHz have shown that, at this frequency, the V^{2+}(II) spectrum is dominated by a line very similar to that with $g = 2.07$ observed in ODMR by Görger *et al* (1988). If the ODMR and TD-EPR lines result from the same centre, then V^{2+}(II) is not isolated. It can be a complex in which one of the As nearest-neighbour sites is vacant (or is replaced by another atom or ion) with a V^{2+} ion at the centre.

The aim of this paper is to present these new TD-EPR 35 GHz results including

studies of photoinduced effects on the spectra. A trigonal model for the V^{2+}(II) centre will also be described and it will be used to provide a possible theory for the original TD-EPR measurements between 8.0 and 12.4 GHz and the new 35 GHz results presented here.

2. Background to previous TD-EPR work on the V^{2+}(II) centre

Our previous TD-EPR measurements, carried out at X-band, on different crystals of GaAs doped with vanadium made by the liquid-encapsulated Czochralski (LEC) or horizontal Bridgman (HB) techniques, gave spectra that exhibit the same set of resonances, which were interpreted as arising from the V^{2+}(II) ion. The lines are either created or enhanced by illumination with a suitable energy. Detailed studies of the variation of the line positions with both the direction of the magnetic field and the quantum size between 8.0 and 12.4 GHz have been made. The results show that V^{2+}(II) is very strongly coupled to the lattice and that the resonances observed are mainly induced by the radio frequency (RF) electric field. The associated symmetry is not obvious from the dependence of the spectra on the direction of the magnetic field. However, it is clear from the spectra observed at different quanta that there are at least three small zero-field splittings, with one of them being the sum of the other two (Vasson *et al* 1984, En-Naqadi 1986, En-Naqadi *et al* 1988). A similar V^{2+}(II) centre has also been detected by TD-EPR in GaP (Vasson *et al* 1984, En-Naqadi 1986, Tebbal 1991).

In En-Naqadi *et al* (1988) we modelled our V^{2+} centre in GaAs by three very closely spaced Kramers doublets, which are split by the magnetic field, within a $^4T_1$ ground state. It was necessary to infer that the ground state was $^4T_1$ and not ^2E because the latter would not generate the required large number of transitions observed in the TD-EPR spectra that relate to the *same* centre. These three Kramers doublets were described by an effective spin of $S' = 5/2$.

The specific model chosen was one in which random strains of orthorhombic symmetry are present, and that these are superimposed on a V^{2+} ion at a site of symmetry T_d. (Orthorhombic symmetry was chosen because it resembled most closely the isoelectronic Cr^{3+} ion in GaAs, which clearly has orthorhombic symmetry as deduced from the conventional EPR measurements of Krebs and Stauss (1977) and the TD-EPR measurements of Parker *et al* (1990)). It seemed appropriate to include random strains because the experiments clearly showed that the centre is strongly coupled to the surrounding lattice as the TD-EPR signals were very strong. The spin Hamiltonian used incorporated these strains in the form of spin operators. The observed resonances were then fitted to the theory by varying the effective g-value and the two strain parameters using the condition that the resonances occur where the product of the transition probability intensity and the strain distribution function is a maximum. Although the major peaks in the TD-EPR spectra were explained, the model was very complicated to interpret in that the random strain played a crucial role as it was different for each transition.

In En-Naqadi *et al* (1988), it was also suggested that an alternative treatment of the V^{2+}(II) centre in GaAs would be to consider it as a V^{2+} ion substituting for a Ga ion at the centre of a tetrahedron in which one of the As sites is left vacant. Such associates or complexes are well known (e.g., Cr^{2+}–V_{As} where V_{As} refers to a vacancy at an arsenic site in GaAs). The ion at the centre feels the effects of

a trigonal field acting along one of the bond directions with an equal probability for each direction. This problem is itself very complicated; the ion in this case would be subjected to a strong dynamic Jahn–Teller (JT) effect, which would quench the trigonal field particularly if it was of a $T \otimes e$ type (Simpson *et al* 1990, 1991). Random strains would also exist but as a trigonal field is already present from the vacancy it is necessary to include strains of e-type symmetry only.

In the next section (section 3) of this paper, results will be presented for this V^{2+}(II) centre for a quantum of order 35 GHz. The following section (section 4) gives details of the 'trigonal model'. It is then used to provide an explanation for the experimental results by obtaining values for the parameters which appear in the model.

3. The TD-EPR experimental results

Before describing our investigations carried out at 35 GHz, it should be noted that further experiments have also been undertaken between 8 and 12.4 GHz on new samples of GaAs doped with vanadium from different manufacturers than those quoted in the experiments described in Vasson *et al* (1984), Ulrici *et al* (1987) and En-Naqadi *et al* (1988). From all these results it can be concluded that *all* the samples studied, from five different manufacturers, exhibit the set of TD-EPR lines attributed to V^{2+}(II) centres. The spectra are either seen in the samples 'as-received' or they are created by illumination depending on the Fermi level position. The first situation occurs in n-type samples (the V^{2+}(II) spectrum is amplified or unaffected by the illumination) and the second situation in semi-insulating samples. The V^{2+}(II) spectrum is only observed in samples containing vanadium. It must be noted that it has been seen in a titanium-doped GaAs sample (Tebbal *et al* 1990) but subsequent SIMS analysis revealed that this sample also contains some vanadium as an impurity as well as titanium. All the results confirm that the centre responsible for the V^{2+}(II) spectra is really vanadium and that it must be divalent with a $^4T_1$ ground state. Furthermore, thermally detected optical absorption (TD-OA) experiments (the method is described in Nakib *et al* 1988) have shown that there is an excellent correspondence between the presence of the isolated V^{2+} TD-OA main signal and the V^{2+}(II) TD-EPR spectra in the samples.

3.1. Experimental details

In order to obtain further information about 3d ions that are strongly coupled to the lattice, in III–V crystals, a 35 GHz TD-EPR spectrometer has been used (e.g., Handley *et al* 1990). As at X-band, the temperature rise of the sample owing to resonance is detected by a carbon glass thermometer at liquid helium temperatures. A halogen lamp, interference filters and optical fibres allow the effects of the illumination on the TD-EPR signals to be studied.

Two samples of GaAs doped with vanadium, one semi-insulating and one n-type, have been investigated at 35 GHz. Here we shall concentrate on the results obtained with the semi-insulating crystal in which both V^{3+} and V^{2+} ions can be studied together in order to compare their behaviour (vanadium concentration about 3.4×10^{16} cm^{-3}). This sample was manufactured by Wacker Chemitronic and was labelled Wa1 in Vasson *et al* (1984) and W1 in En-Naqadi *et al* (1988).

3.2. Typical TD-EPR spectra

Figure 1 shows the spectra obtained in the dark both before and after illumination when the magnetic field B is parallel to the [001] axis. In agreement with the result previously reported (Vasson *et al* 1984), the V^{3+} signal is observed before illumination. However, it is much clearer at 35 GHz than at 10 GHz. Its shape and g-value are the same as those obtained in conventional EPR (Kaufmann *et al* 1982) experiments and in ODMR (Görger *et al* 1988) experiments for the V^{3+} ion in GaAs. Furthermore, the study of its intensity as a function of the microwave power confirms that the ion responsible is weakly coupled to the lattice.

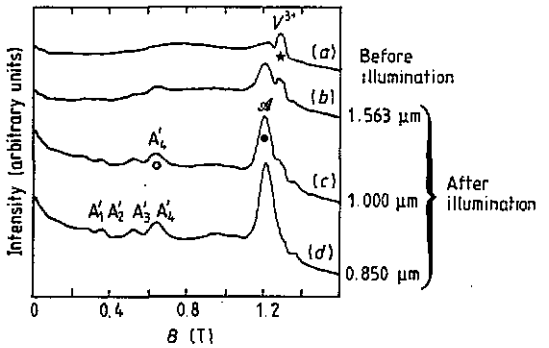

Figure 1. Thermally detected EPR spectra of GaAs:V at 34.85 GHz for B parallel to the [001] axis showing the V^{3+} line before illumination (a) and the decrease of its intensity together with the emergence of the V^{2+}(II) signals (A'_n and $\mathcal{A}$) after illumination with a photon energy of $h\nu_{exc}$ = 0.79 eV (b), 1.24 eV (c) and 1.46 eV (d). The line labelled by $\mathcal{J}$ arises from the alumina sample holder.

After illumination the V^{3+} line decreases in intensity and the V^{2+}(II) signals appear (labelled by A'_n in figure 1, where n = 1,2,3,...). The most intense line, $\mathcal{A}$, created by the illumination is observed near g = 2.07. It is very similar to the isotropic ODMR signal of Görger *et al* (1988), which was attributed, by these authors, to a V^{2+} centre. However, the $\mathcal{A}$ line is only intense when B is near the [001] axis. As the magnetic field moves away from this axis the intensity of this line rapidly decreases and an overlap with other resonances occurs.

The V^{2+}(II) isofrequency diagram for B in the $(1\bar{1}0)$ plane is shown in figure 2.

3.3. Microwave power dependences of the signals and decay times

In order to know if the $\mathcal{A}$ line can be due to V^{2+}(II) the spectra have been investigated with different values for the microwave power P_{RF} (see figure 3). The variations of the intensities of the A_n and $\mathcal{A}$ lines with P_{RF} coincide. The results indicate that all these lines are strongly coupled to the lattice with similar strengths so that they arise from the same centre.

The decays of the A_n and $\mathcal{A}$ signals and the recovery of the V^{3+} line have also been studied. They all lead to a time constant of the order of 10^6 s.

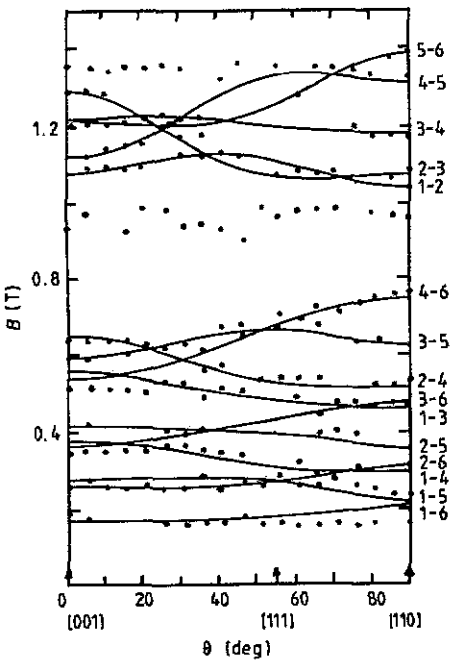

Figure 2. Experimental isofrequency diagram for V^{2+}(II) in the $(1\bar{1}0)$ plane, at 34.85 GHz, together with theoretical curves calculated using the 'trigonal' model in the zero-strain approximation (see section 4.2.2). Only the graphs obtained for sites 2 and 3 (which coincide) are shown for clarity.

3.4. Photoinduced effects on the V^{3+} and V^{2+} signals

The effects of illumination have been studied at both X- and Q-bands. The spectral dependences (amplitudes of the signals plotted against the size of the illumination quantum $h\nu_{exc}$) have been measured. The experiments have been carried out in two different ways; the first method involves starting with the smallest quantum available (0.79 eV) as in Tebbal *et al* (1990) and increasing $h\nu_{exc}$ and in the second method we start by bleaching out $EL2^0$ as described in Ulrici *et al* (1987) (using 0.79 eV instead of 0.75 eV to restore the vanadium signal). The spectral dependences for the A_4', $\mathcal{A}$ and V^{3+} lines are shown in figure 4(*a*) at 35 GHz (using the first process for the illumination). Already at 0.79 eV, the A_4' and $\mathcal{A}$ lines have appeared and the V^{3+} line is smaller than it was prior to illumination. When $h\nu_{exc}$ increases, the creation and amplification of the A_4' and $\mathcal{A}$ signals are in good agreement with the decrease of the V^{3+} line. The curves of figure 4(*a*) all exhibit two onsets at 1.03 and 1.38 eV. The onset of 1.03 eV was also observed in the spectral dependences of the conventional EPR and OA signals of V^{3+} in n-type GaAs:V samples (Ulrici *et al* 1987).

The same two onsets have been obtained at 10 GHz for semi-insulating and n-type crystals (Tebbal 1991). Figure 4(*b*) gives an example of the spectral dependence of a line of V^{2+}(II) in W1, at this frequency, with the second process of illumination. In this case the change in the spectrum at 0.79 eV, with respect to that before illumination, is much less than that observed with the first process.

To explain the illumination effects for $h\nu_{exc}$ = 0.79 eV, the following photoionization processes can be expected with an onset at about 0.75 eV corresponding to the

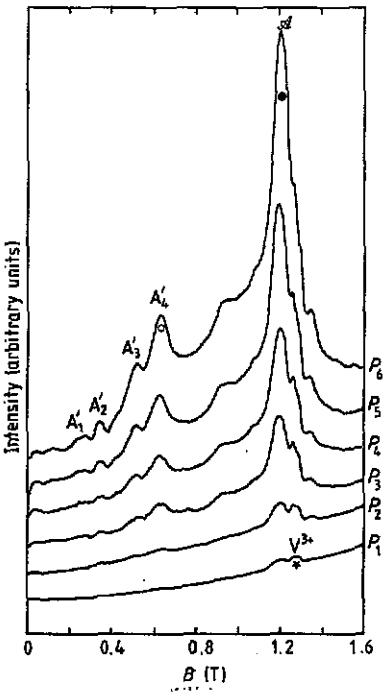

Figure 3. Evolution with the microwave power P_{RF} of the thermally detected EPR spectrum of GaAs:V at 34.85 GHz, after illumination with light of energy $h\nu_{exc} = 1.13$ eV. This figure shows the saturation of the V^{3+} (*) signal and the increase of the intensities of the V^{2+}(II) (A_n and A) lines with P_{RF} ($P_{RF} = P_n$, $n = 1, 2 \ldots, P_1 < P_3 < P_4 \ldots$). ($A'_4$: O; A: ●).

$EL2^+/EL2^0$ level:

$$EL2^0 + h\nu_{exc \geqslant 0.75eV} \rightarrow EL2^+ + e^-_{cb} \tag{3.1a}$$

$$V^{3+}(II) + e^-_{cb} \rightarrow V^{2+}(II) \tag{3.1b}$$

$$V^{3+} + e^-_{cb} \rightarrow V^{2+} \tag{3.1c}$$

where e^-_{cb} is an electron in the conduction band. Similarly, for the effects of the illumination with an onset at about 1.03 eV we can have:

$$EL2^+ + h\nu_{exc \geqslant 1.01eV} \rightarrow EL2^{2+} + e^-_{cb} \tag{3.2a}$$

(with the $EL2^+/EL2^{2+}$ level at $E_v + 0.51$ eV) or

$$Fe^{2+} + h\nu_{exc \geqslant 1.03eV} \rightarrow Fe^{3+} + e^-_{cb} \tag{3.2b}$$

(with the Fe^{2+}/Fe^{3+} level at $E_v + 0.49$ eV; Shanabrook *et al* (1983)) followed by the capture of e^-_{cb} by V^{3+}(II) or by the isolated V^{3+} ion as in (3.1*c*). (Fe is the usual contaminant in GaAs:V samples. Its concentration in W1 is between 2 and 3 × 10^{16} cm^{-3}.) However, the absorption cross-section of the process involving Fe is very small (Kleverman *et al* 1983) so that its efficiency is not expected to be very high. The recharging involving $EL2^+$ appears to be the most probable.

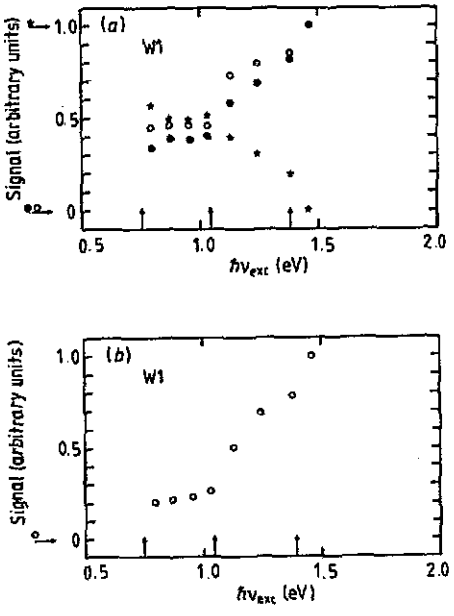

Figure 4. Dependences of the photoinduced changes of the TD-EPR signals on illumination energy (B along the [001] axis): (*a*), for the V^{3+} (*) and V^{2+}(II) ions (A_4': O; A: ●) at 34.85 GHz; (*b*) for the V^{2+}(II) ion at 10 GHz for comparison. The amplitudes of the signals measured before illumination are indicated on the left-hand side by the horizontal arrows. The onsets of the photoionization processes are shown by the vertical arrows.

The third onset at about 1.38 eV corresponds to the isolated V^{3+}/V^{2+} level positioned at $E_c - 0.14$ eV, so that

$$V^{3+} + h\nu_{exc \geq 1.38eV} \rightarrow V^{2+} + h_{vb}^{+} \tag{3.3}$$

where h_{vb}^{+} is a hole in the valence band. If V^{2+}(II) is part of a complex we must also have the following process:

$$V^{3+}(II) + h\nu_{exc \geq 1.38\ eV} \rightarrow V^{2+}(II) + h_{vb}^{+} \tag{3.4}$$

with the $V^{3+}(II)/V^{2+}(II)$ level very close to the V^{3+}/V^{2+} level. It must be emphasized that the 1.38 eV onset has also been seen on the spectral dependences of the V^{2+}(II) TD-EPR signals obtained at 10 GHz for n-type samples, which exhibit illumination effects.

3.5. Further comments on the $g = 2.07$ ODMR and the TD-EPR A line

From the experimental results reported here, it appears that the V^{3+} and V^{2+}(II) ions responsible for the TD-EPR signals can be two charge states of the same vanadium ion. Information that could distinguish between V^{2+}(II) being an isolated ion or part of a complex can be obtained by determining whether or not the $g = 2.07$ ODMR line and the TD-EPR line (labelled A), which can be attributed to V^{2+}(II), are due to the same ion. They look very similar. Nevertheless, some differences in their behaviour

seem to occur. Firstly, the ODMR signal is reported to be isotropic (Görger *et al* 1988). Secondly, the intensity of the A line depends strongly upon the orientation of the sample in the magnetic field and, because of its overlap with other lines, it is difficult to establish accurately whether or not its real position alters as B is rotated away from the [100] direction. However, it must not be forgotten that the TD-EPR V^{2+}(II) lines are mainly induced by RF electric fields (Vasson *et al* 1984). This means that the line A can appear to behave differently from the ODMR line even if they both arise from the same V^{2+} centre. Another difference is that the spectral dependence of the MCD signal, corresponding to the ODMR line, exhibits only one onset, which is different from those observed in photo-TD-EPR. However, the samples studied by the two techniques are not from the same manufacturer. Thus it is possible that the two lines can be attributed to the same centre although it is difficult to prove this categorically.

As stated above, if the centres *are* the same, they must be labelled as V^{2+}(II) with the V^{2+} ion itself forming part of a complex. With such a conclusion, the simplest case is that of a V^{2+} ion associated with an As vacancy (or with another defect replacing As) which creates a trigonal field at the V^{2+} site. In the next section we shall consider such a model for V^{2+}(II), in order to test the hypothesis that V^{2+}(II) is such a complex.

4. The trigonal model

The expected ground state of the V^{2+} ion investigated here in a tetrahedral field is $^4T_1$. One approximation is to treat the trigonal field as a perturbation to be added after the ion–lattice coupling, which generates the JT effect. It is then a purely orbital operator to be considered alongside the spin–orbit coupling. The JT effect converts the orbital part of the ground state to a vibronic part in which the symmetry remains as $^4T_1$ whatever the nature (either $T \otimes e$, $T \otimes t_2$ or $T \otimes (e + t_2)$) of the JT effect. The ground state will be split by the trigonal field and spin–orbit coupling acting together, after the insertion of appropriate reduction factors in front of each term and the inclusion of second-order JT terms. Thus we suppose that the effective sizes of the spin–orbit and trigonal perturbations are approximately equal. This results in the formation of six Kramers doublets with separations dependent upon the sizes of the spin–orbit constant, the trigonal-field parameter and the reduction factors. It is impossible to predict the magnitude of the splittings of these doublets from theory alone and thus it is necessary to turn to the experimental results for the required information.

In the case of V^{2+}(II) in GaAs there appear to be three very closely spaced Kramers doublets, which are separate from the other three doublets. A convenient method of study therefore is to model these doublets together with an effective spin S of 5/2, as in En-Naqadi *et al* (1988). (From the recent work of Simpson *et al* (1990, 1991), a more accurate modelling would be achieved if the trigonal field was regarded as part of the JT effect itself. However, the formalism resulting from such a modelling in terms of an effective spin could not be distinguished from the simpler case discussed here.)

4.1. The spin Hamiltonian

There are four equivalent directions for the trigonal field created by the vacancy within the cluster namely $[1\bar{1}\bar{1}]$, $[\bar{1}\bar{1}\bar{1}]$, $[\bar{1}1\bar{1}]$ and $[\bar{1}\bar{1}1]$. The corresponding sites are

labelled 1, 2, 3 and 4 respectively (figure 5). For certain directions of the magnetic field, some of the sites are magnetically equivalent. The Hamiltonian $\mathcal{H}_{trig}$ for the trigonal field for site 1 is given by

$$\mathcal{H}_{trig} = \mathcal{H}_X + \mathcal{H}_Y + \mathcal{H}_Z \tag{4.1a}$$

where

$$\mathcal{H}_X = E(S_y S_z + S_z S_y) \tag{4.1b}$$

etc, where E is the trigonal parameter.

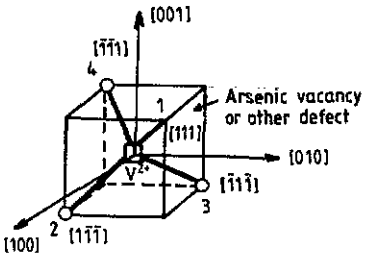

Figure 5. A trigonal V^{2+} centre

The corresponding Hamiltonians for sites 2, 3 and 4 may be obtained directly from (4.1) by adding in the appropriate signs, namely $+--$, $-+-$, $--+$ respectively, in front of $\mathcal{H}_X$, $\mathcal{H}_Y$ and $\mathcal{H}_Z$.

Random strains have many components, which may be grouped under the labels A_1, E, T_1 and T_2 in T_d symmetry. As the T_2 strains are much smaller than the trigonal field, which is also of T_2 symmetry, they may be neglected. Thus the only strains of interest to cause splittings within the vibronic ground state are those of E-type. The E-type Q_θ random strain for the site 1 can be written in the form

$$\mathcal{H}_D = D[3S_z^2 - S(S+1)] \tag{4.2}$$

where D is the strain parameter. Strains along the [001], [010] and [100] axes are equivalent to each other for trigonal sites. (It is unnecessary to consider the other component Q_ϵ of the E-type strain for symmetry reasons.)

It is also necessary to add the cubic term (from fourth-order spin–orbit coupling),

$$\mathcal{H}_A = A[S_x^4 + S_y^4 + S_z^4 - \tfrac{1}{5}S(S+1)(3S^2+3S-1)] \tag{4.3}$$

and the Zeeman term

$$\mathcal{H}_B = g\mu_B B \cdot S. \tag{4.4}$$

Thus the total Hamiltonian is given by

$$\mathcal{H}_{spin} = (\mathcal{H}_X + \mathcal{H}_Y + \mathcal{H}_Z) + \mathcal{H}_D + \mathcal{H}_A + \mathcal{H}_B \tag{4.5}$$

for the sites 1 with corresponding expressions for the other sites.

4.2. Fitting to the data

Two procedures have been adopted to fit the TD-EPR data. The first method is appropriate for data obtained at X-band. It resembles that devised by En-Naqadi *et al* (1988) for the orthorhombic model, in which the maximum of the product of the transition probability and the strain distribution function gives a peak in the resonance spectrum. A peak will be obtained when the resonance condition is satisfied for a particular relatively small value of the strain. The aim will be to predict the peak positions in calculating their maximum intensities and the corresponding values for the strain consistent with the zero-field splittings found from the frequency-dependence data reported in Vasson *et al* (1984) and En-Naqadi *et al* (1988). As in the latter paper the transition probabilities for the electric-field-induced transitions, which dominate for V^{2+}(II), will be computed. In the second method, appropriate for the larger quantum of 35 GHz, the effect of the strain will be ignored. Values for the fixed parameters will be obtained, which gave the best fit to the zero-field splittings and the isofrequency curves.

4.2.1. Fitting to the spectra obtained at X-band: the transition probabilities. The first step is to find values for the constant parameters E and A and the allowed range of values for the variable parameter D that fit the zero-field splittings of 4.0 and 13.5 GHz. This is achieved by, firstly, equating the differences between the diagonal elements of the zero-field 6×6 matrix from $\mathcal{H}_{\text{spin}} - \mathcal{H}_B$ to these splittings making a self-consistent choice. This gives

$$|D| < 1 \text{ GHz} \qquad |A| < 5 \text{ GHz}.$$

A computer program is then used, taking into account all the matrix elements, to find precise values for E and A to reproduce the observed zero-field splittings as D was varied between 1.2 and -1.2 GHz. It is found that the zero-field splittings of 4.0 $\pm$ 2.0 and 13.1 $\pm$ 0.5 GHz are predicted by the following:

$$E = 0.90 \pm 0.04 \text{ GHz}$$

$$A = -0.28 \pm 0.09 \text{ GHz}$$

and

$$-0.04 \leqslant D \leqslant 0.45 \text{ GHz}.$$

These zero-field splittings are within the range found experimentally when possible curving near the v-axis of the B–v lines is taken into account where v is the microwave frequency.

The value taken for $g_{\|}$ was the same as that used in the orthorhombic model, namely $g_{\|} = 1.65 \pm 0.15$. The parameters E and A were kept at the constant values above while D was varied over the quoted range in order to obtain the value of the magnetic field at which the intensity of the transition was a maximum at the given frequency. It was also assumed that the strain distribution function remained flat over the range of strains considered. The intensities of the transitions were calculated for two directions, namely parallel (Oz) and perpendicular (Ox), of the magnetic field and at frequencies between 8.53 and 12.00 GHz. As an example table 1 gives the values obtained for D for a frequency of 10.32 GHz in terms of the transitions

Table 1. Details of the predicted peaks at 10.32 GHz

B (T)	Transition	D (GHz)	Intensity (arbitrary units)
0.061	4–5 z	−0.23	0.70
0.067	1–4 z	−0.38	0.95
0.097	1–4 x	0.07	2.53
0.116	3–5 x	0.05	6.29
0.128	3–5 z	0.06	0.65
0.139	1–3 x	0.20	2.17
0.150	2–4 x	−0.30	5.31
0.184	5–6 z	−0.03	3.00
0.185	5–6 x	0.09	0.97
0.217	2–4 z	−0.27	0.66
0.217	1–3 z	0.27	3.87
0.298	1–2 z	0.02	1.84
0.298	1–2 x	−0.04	2.40
0.411	4–5 x	0.12	2.03
0.496	3–4 x	−0.36	3.34
0.507	2–3 x	0.23	1.01
0.528	2–3 z	−0.03	1.70

involved (labelled by the energies of the levels at the given magnetic field with '1' as the lowest), the direction (along x or z) of the magnetic field and its magnitude. Intensities less than 0.5 (in relative units) have been excluded from the table.

As in the case of the orthorhombic model the calculated values of D vary with the transition involved and also with the frequency. A comparison of these results with the observed TD-EPR spectrum for B along [001] at this frequency of 10.32 GHz is shown in figure 6.

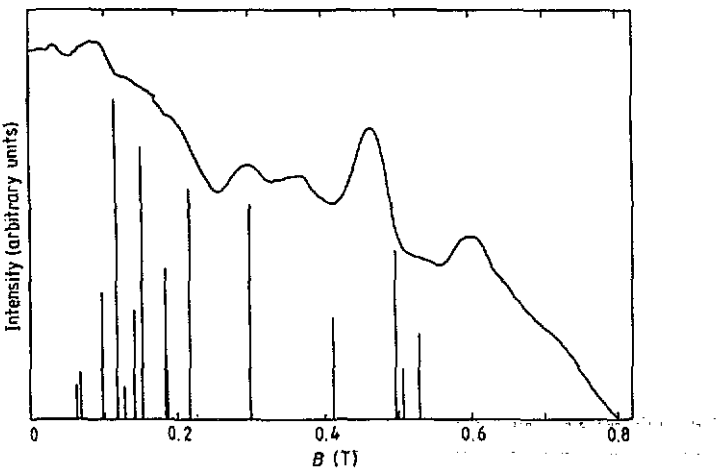

Figure 6. A comparison of an experimental spectrum with the predicted peaks at 10.32 GHz for B parallel to the [001] axis.

Many other similar sets of results have been obtained throughout the frequency range studied and all have the general characteristics shown in table 1 and figure 6. However, it should be noted that as the peaks have a finite width a significant amount

of overlapping of the various transitions occurs. Reasonable agreement has been obtained between the computer predictions and experiment for the peaks considered in detail. In addition, the model predicts that there are no peaks present at fields higher than those observed in the experiments in all the cases considered. Detailed results are given in Labadz (1987).

4.2.2. Isofrequency curves at Q-band: the zero-strain approximation. From the above, it is clear that the strain parameter D varies as the direction of the magnetic field changes. This presents an enormous problem for the fitting to the isofrequency curves. To proceed therefore a further approximation is needed, for instance, by neglecting the strain completely. Thus D was taken to be zero in such a model. This approximation is justified at 35 GHz because the change in energy from the strain is then a smaller fraction of the quantum than it was at X-band.

With this hypothesis a numerical analysis of the spin Hamiltonian has been undertaken to obtain values for E and A which are the best fit to the zero-field splittings deduced from the B–v data, namely:

$$E = 0.952 \text{ GHz} \qquad A = -0.188 \text{ GHz}.$$

Note that these values are near the values used in section 4.2.1 above.

The best fit to the Zeeman data was obtained by taking $g_{\parallel} = g_{\perp} = 2.07$; this value corresponds to the most intense peak A observed at 1.2 T using a frequency of 34.85 GHz. The calculated isofrequency graphs for the magnetically equivalent sites 2 and 3 deduced from this set of parameters are shown in figure 2 together with the experimental points. The curves are labelled with the transition involved. These results show that there is reasonable agreement between the calculated and observed isofrequency curves for these sites. Figure 7 shows the corresponding energy level diagram for the V^{2+}(II) ions in GaAs for B along the [001] axis.

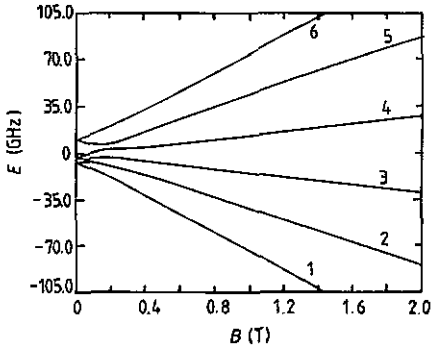

Figure 7. Splitting of the energy levels labelled 1 to 6 of V^{2+}(II) in the 'trigonal' model when B is parallel to the [001] axis for the zero-strain case.

4.2.3. The spin Hamiltonian g-values. It is worth noting that the g-values obtained here describe the relative slopes of the Zeeman-split levels for energy separations equal to the microwave quantum used. For a smaller quantum, the strain effects are more important than for a higher quantum so that such an effective g-factor must be implicitly dependent on strain. An alternative procedure would be to introduce

an extra term such as $\mu_B \boldsymbol{B} \cdot \mathbf{h} \cdot \boldsymbol{S}$ (e.g., Tucker and Rampton 1972, Clerjaud private communication) where the tensor $\mathbf{h}$ has the components H_{ij} given by

$$H_{ij} = \sum F_{ijkl} \epsilon_{kl}. \tag{4.6}$$

The strain is taken as zero for the larger quantum and thus the term in $\mathbf{h}$ drops out of the calculation. In this case (35 GHz), we thus obtain for g the real g-value which is independent of strain. However, for the smaller quantum the strain is finite but variable and thus the effective g-value of 1.65 ± 0.15 should be the sum of the strain-independent g added to the contribution from the strain-dependent $\mathbf{h}$. In the spectra fitted it is impossible to separate g from $\mathbf{h}$. It is then not surprising therefore that the required g-values to be inserted in the spin Hamiltonian we have used (4.5) are not the same at about 10 GHz (g = 1.65) and at 35 GHz (g = 2.07). For low microwave energies the g-values corresponding to this spin Hamiltonian are different from those used in the formalism of the effective Hamiltonian. (The latter can be written in a similar way to that given in Dunn *et al* (1986) and Parker *et al* (1990) for the isoelectronic Cr^{3+} ion in GaP and GaAs respectively.) It would also be anticipated that when the microwave quantum increases, the g-value needed in the spin Hamiltonian would tend towards that required in the effective Hamiltonian which is the real g.

5. Discussion and conclusions

5.1. Conclusions from the TD-EPR experiments

The TD-EPR spectra, consisting of a set of overlapping resonances, described above and in our earlier papers undoubtedly result from vanadium. They are only observed in n-type samples known to contain vanadium. They are created by illumination in the semi-insulating specimens and seen in the other samples in their 'as-received' state. A correspondence between their presence and that of the isolated V^{2+} ion has been noted. The TD-EPR lines are very intense and dominate virtually all the other impurities that may be present. Consistent with this observation are the large line widths associated with the resonances. This implies that in any modelling strong JT effects are expected and that random strains will also be important. All the TD-EPR results show that the centre responsible must be a V^{2+} ion with a $^4T_1$ ground state. It has been labelled as V^{2+}(II).

The isofrequency curves associated with V^{2+}(II) at both X- and Q-bands do not reflect a symmetry that is easy to identify. However, other measurements carried out in both frequency ranges have given interesting information about this centre. The small zero-field splittings deduced from the previously reported frequency dependences at X-band have shown that its lowest states consist of three Kramers doublets. The investigations at 35 GHz in a semi-insulating sample described here have given us the opportunity of studying V^{3+} and V^{2+}(II) together, and simultaneously, to detect a line labelled A similar to that seen in ODMR and also attributed to a V^{2+} centre by Görger *et al* (1988). From the analysis of the decay times of the illumination effects and of the microwave power and spectral dependences of the TD-EPR lines, it can be concluded that:

(i) the A line arises from V^{2+}(II) (in fact, it is dominated by V^{2+}(II), as it is not a single resonance).

(ii) there is an excellent correlation between the behaviour of the V^{3+} signal and those of V^{2+}(II), and

(iii) the V^{2+}(II)/V^{3+}(II) level is very close in energy to the isolated acceptor level.

From these results, the question 'Is V^{2+}(II) a complex or the isolated V^{2+} ion?' arises again. We shall consider these two possibilities successively.

5.2. *The V^{2+}(II) complex*

Bearing in mind the first point (i) in particular and also the fact that the $\mathcal{A}$ and ODMR V^{2+} lines result from the same type of V^{2+} ion, namely V^{2+}(II), we have tried a 'trigonal' model for V^{2+}(II) in which it is associated with a defect at a near-neighbour As site (an As vacancy or another defect substituting for As). The three lowest very closely spaced Kramers doublets have been described by an effective spin of 5/2, which incorporates spin–orbit coupling and the trigonal field created by the defect. The observed spectra are thus a superposition of signals from all four sites with a multitude of possible transitions between the magnetic-field-split levels. The energy level pattern is quite different from that of the isoelectronic Cr^{3+} ion in GaAs chiefly because the Kramers doublets are much closer together.

The model used in the analyses above is dominated by strain for measurements taken at around 10 GHz. For these frequencies, the various resonances are much wider than the energy equivalent of the separation between the levels. Thus the interpretation of the different lines is necessarily very complicated. At around 35 GHz the quantum is sufficiently large that strain effects can be neglected, thus resulting in a much clearer model for the spectra and the angular dependence.

It is probable that the V^{2+}(II) spectra dominates that from the isolated V^{2+} ion if the latter has a ^2E ground state that is much less strongly coupled to the lattice than $^4T_1$ (Butler *et al* 1989). In addition, for GaAs much stronger resonances from complexes than from isolated ions are expected in line with observations of other complexes (e.g., Cr^{2+}–V_{As}) and theoretical predictions (Polinger *et al* 1992).

The second and third points (ii) and (iii) above follow on logically even if V^{2+}(II) is identified as a complex. The same onsets observed for the photoinduced effects for both V^{3+} and V^{2+}(II) can be explained by photoionization processes involving the creation of electrons trapped by V^{3+} and V^{3+}(II) and by the closeness of the V^{2+}/V^{3+} and V^{2+}(II)/V^{3+}(II) levels. The latter is in agreement with the electrical properties.

5.3. *The isolated V^{2+} ion*

Values for the parameters that appear in the trigonal model have been obtained above that fit the calculated transition probabilities to the X-band spectra and the calculated zero-strain resonances to the experimental isofrequency curves at Q-band. The results are therefore satisfactorily explained by the trigonal model and the assumption that V^{2+}(II) is a complex. However, these results do not *prove* absolutely that V^2(II) is such a complex. Furthermore, it is not certain that the $\mathcal{A}$ line results from the same centre as that responsible for the ODMR line. As stated above we have observed some discrepancies between the behaviour of the two signals. If the ODMR line is *not* attributable to V^{2+}(II) (such a deduction is indeed possible), why cannot the V^{2+} centre, giving rise to the TD-EPR signal, be the isolated V^{2+} ion? All our TD-EPR results are in agreement with this interpretation. However, the main problem is the exact nature of the ground state of the isolated V^{2+} ion. In the hypothesis

adopted by a majority of authors the ground state is expected to be ^2E, whereas our V^{2+}(II) centre certainly has a $^4T_1$ ground state. We know of three papers cited previously describing experiments that are reported to favour the low-spin ground state, namely ODMR (Görger *et al* 1988), DLOS (Bremond *et al* 1989) and phonon scattering measurements (Butler *et al* 1989). We discuss and comment on these results now.

In our opinion, and consistent with the discussion above, the V^{2+} centre detected by ODMR is not isolated. Thus this does not affect in any way our conclusions for V^{2+}(II) if they are different ions with our present hypothesis. (We note in passing that the statement in Görger *et al* (1988), which infers that the peak that they observe in their ODMR experiments with $g = 2.07 \pm 0.02$ is related to the ^2E ground state because it is described by an effective spin of $S' = \frac{1}{2}$, is invalid. Although it is obviously straightforward to relate the spin $S' = \frac{1}{2}$ to the ^2E ground state of the isolated V^{2+} ion, it is equally appropriate to relate it to a $^4T_1$ ground state.) Bremond *et al* (1989) have adopted the ^2E ground state for isolated V^{2+} on account of the very weak photoionization scattering cross section σ_n^0 of the isolated vanadium acceptor level as measured by DLOS. Their deduction is based on a comparison of the experimental results and theoretical values of σ_n^0 for the 3d ion levels from GaAs with those from InP (Delerue *et al* 1988). Thus it appears that the phonon scattering experiments of Butler *et al* (1989) and Sahraoui-Tahar *et al* (1989) on vanadium-doped GaAs, GaP and InP represent the only direct experimental proof that the ground state is ^2E in GaAs and $^4T_1$ in GaP (V^{2+} does not exist in any form in InP).

Further discussion is necessary particularly on photoinduced effects in the different experiments. Butler *et al* (1989) assigned the TD-EPR (and APR) signals to V^{2+} complexes because of the difference (the decay times and the optical frequency dependence) in the photoinduced effects observed in TD-EPR (and APR) and in optical absorption (Ulrici *et al* 1987). The decay times appear to be much shorter for the optical signal attributed to the isolated ion than for the V^{2+}(II) TD-EPR (and APR) lines. However, additional infrared irradiation can involve effects that may depend on the type of probe used. Only a difference in the decay times measured during the *same experiment* is relevant. It must be emphasized that, in our TD-EPR investigations at 35 GHz, we have obtained the same decay time of the illumination effects for both V^{3+} and V^{2+}(II). In addition, it was found that the V^2(II) signals detected in both TD-EPR and APR were sensitive to illumination within the range $0.7 \leqslant h\nu_{exc} \leqslant 1.5$ eV, whereas the photoinduced effects in OA and in the EPR from V^{3+} ions (Ulrici *et al* 1987) were only observed for values of $h\nu$ larger than about 1.0 eV. However, the measurements of Ulrici *et al* (1987) were made *after* the removal of $EL2^0$ (section 3), whereas in the previous experiments on V^{2+}(II) the $EL2^0$ defects were not bleached away. We have seen above that the illumination effects on the V^{2+}(II) TD-EPR lines are different in the two illumination processes. Thus these differences in the spectral dependences do not prove that V^{2+}(II) is part of a complex. Furthermore, the strength of the low-frequency phonon scattering may indicate that the concentration of this centre is quite high (Butler *et al* 1989). These authors conclude that this low-frequency phonon scattering results from V^{2+}(II) ions, as the resolved peaks coincide with the zero-field splittings observed in TD-EPR.

5.4. Summary

The JT model with orthorhombic strains described by En-Naqadi *et al* (1988) can be used if V^{2+}(II) is isolated. It leads to a reasonable fit to the X-band spectra when

the transition probability calculations are taken into account. However, although the orthorhombic model appears to give a better fit than the trigonal model, it is critically dependent upon the input parameters and thus much less convincing from a theoretical point of view. The calculated parameters were chosen to fit the experimental data directly. In contrast, in the trigonal model described here, the peak positions at X-band were predicted and the results compared directly with the experiments. In addition, the conditions that generate the orthorhombic JT effect for the isoelectronic Cr^{3+} ion in GaAs are rather special and there is no direct experimental evidence that the same situation occurs with V^{2+}.

The first interpretation that V^{2+}(II) is a complex was due, in part, to its high spin configuration in contrast to a theoretical prediction that the isolated V^{2+} ion in GaAs had a ^2E ground state. However, in considering all our TD-EPR results, particularly those obtained at 35 GHz, the conclusion that V^{2+}(II) is really isolated V^{2+} cannot be ruled out if the TD-EPR and ODMR lines are not due to the same centre. Before a definitive identification of V^{2+}(II) in GaAs can be made the problem of V^{2+}(II) in GaP must be considered in detail. As the behaviour of the TD-EPR lines is very similar to that in GaAs it is logical to attribute them to the same V^{2+} ion. The work on GaP:V will be reported in the near future (Vasson *et al* 1992).

Nevertheless, if V^{2+}(II) is *not* a complex, it implies that the isolated V^{2+} ion has a $^4T_1$ ground state as deduced for this ion in GaP (Sahraoui-Tahar *et al* 1989). However, the very strong, high-frequency phonon scattering that is observed in GaP and attributed to the $^4T_2$–$^4T_1$ inversion splitting associated with a very strong orthorhombic JT effect, is completely absent in GaAs. It would be very surprising if the weaker phonon scattering, which is observed at a much lower frequency in GaAs, would be the equivalent inversion splitting as it would be considerably smaller and in marked contrast with all other experimental data observed by phonon scattering on many other orbital triplet and doublet systems in III–V semiconductors (Butler *et al* 1989, Challis private communication). Thus, at this stage, it seems reasonable to retain the conclusion that the V^{2+} centre seen in GaAs by TD-EPR is not the isolated V^{2+} ion. This is in agreement with all the results reported to date. However, further information on V^{2+}(II) centres in GaP and on the comparison of the A and the ODMR lines should enable us to check this identification.

We thus suppose that in GaAs the V^{2+} centre with a $^4T_1$ ground state (observed in TD-EPR) is probably a complex in which one of the As atoms is replaced by a vacancy or other defect. The electrical properties are explained if it is assumed that the V^{3+}/V^{2+} level has an energy very similar to that of the V^{3+}(II)/V^{2+}(II) level. The modelling of this centre has been undertaken with such an hypothesis. In this case, a further question can arise. Is there any relation between V^{2+}(II) and the V^{2+} centre that has gettered a shallow donor impurity as considered by Ko *et al* (1989)?

Acknowledgments

We are particularly grateful to Professors L J Challis, B Clerjaud and W Ulrici, and to Dr J L Dunn, for many helpful discussions about the problem of vanadium, and to many of our other colleagues for their comments. We would also like to thank the EC for a Twinning Grant that was operational when the earlier parts of this work were undertaken and the SERC for a Research Studentship (AFL).

References

Bremond G, Hizem N, Guillot G, Gavand M, Nouailhat A and Ulrici W 1989 *J. Electron. Mater.* **18** 391–7

Butler N, Challis L J, Sahraoui-Tahar M, Salce B and Ulrici W 1989 *J. Phys.: Condens. Matter* **1** 1191–203

Caldas M J, Figueiredo S K and Fazzio A 1986 *Phys. Rev.* B **33** 7102–9

Clerjaud B 1985 *J. Phys. C: Solid State Phys.* **18** 3615–61

Clerjaud B, Naud C, Deveaud B, Lambert B, Plot B, Bremond G, Benjeddou C, Guillot G and Nouailhat A 1985 *J. Appl. Phys.* **58** 4207–15

Delerue C, Lanoo M, Bremond G and Nouailhat A 1989 *Europhys. Lett.* **9** 373–8

Dunn J L, Bates C A, Darcha M, Vasson A and Vasson A-M 1986 *Phys. Rev.* B **33** 2029–32

En-Naqadi M 1986 *PhD Thesis* University of Clermont-Ferrand II

En-Naqadi M, Vasson A, Vasson A-M, Bates C A and Labadz A F 1988 *J. Phys. C: Solid State Phys.* **21** 1137–53

Görger A, Meyer B K, Spaeth J M and Hennel A M 1988 *Semicond. Sci. Technol.* **3** 823–8

Handley J, Bates C A, Vasson A, Vasson A-M, Ferdjani K and Tebbal N 1990 *Semicond. Sci. Technol.* **5** 710–5

Hennel A M, Brandt C D, Ko K Y, Lagowski J and Gatos H C 1987 *J. Appl. Phys.* **62** 163–70

Katayama-Yoshida H and Zunger A 1986 *Phys. Rev.* B **33** 2961–4

Kaufmann U, Ennen H, Schneider J, Wörner R, Weber J and Köhl F 1982 *Phys. Rev.* B **25** 5598–606

Kleverman M, Omling P, Lebedo L A and Grimmeis H G 1983 *J. Appl. Phys.* **54** 814–9

Ko K Y, Lagowski J and Gatos H C 1989 *J. Appl. Phys.* **66** 3309–16

Krebs J J and Stauss G H 1977 *Phys. Rev.* B **15** 17–22

Labadz A F 1987 *PhD Thesis* University of Nottingham

Nakib A, Houbloss S, Vasson A and Vasson A-M 1988 *J. Phys. D: Appl. Phys.* **21** 478–82

Parker L W, Bates C A, Dunn J L, Vasson A and Vasson A-M 1990 *J. Phys.: Condens. Matter* **2** 2841–58

Polinger V Z, Dunn J L and Bates C A 1992 to be published

Rampton V W, Saker M K and Ulrici W 1986 *J. Phys. C: Solid State Phys.* **19** 1037–42

Sahraoui-Tahar M, Salce B, Challis L J, Butler N, Ulrici W and Cockayne B 1989 *J. Phys.: Condens. Matter* **1** 9313–24

Shanabrook B V, Klein P B and Bishop S G 1983 *Physica* B **116** 444–8

Simpson J A L, Bates C A and Dunn J L 1991 *J. Phys.: Condens. Matter* **3** 6845–58

Simpson J A L, Dunn J L and Bates C A 1990 *J. Phys.: Condens. Matter* **2** 8315–26

Tebbal N 1991 *PhD Thesis* University Blaise Pascal-Clermont-Ferrand II

Tebbal N, Vasson A-M, Vasson A, Erramli A and Ulrici W 1990 *J. Phys.: Condens. Matter* **2** 7907–10

Tucker J W and Rampton V W 1972 *Microwave Ultrasonics in Solid State Physics* (Amsterdam: North-Holland)

Ulrici W, Friedland K, Eaves L and Halliday D P 1985 *Phys. Status Solidi* b **131** 719–28

Ulrici W, Kreissl J, Vasson A, Vasson A-M and En-Naqadi M 1987 *Phys. Status Solidi* b **143** 192–206

Vasson A, Vasson A-M, Bates C A and Labadz A F 1984 *J. Phys. C: Solid State Phys.* **17** L837–41

Vasson A, En-Naqadi M and Vasson A-M 1986 *J. Phys. D: Appl. Phys.* **19** 1149–57

Vasson A-M, Vasson A, Gavaix A, Tebbal N, En-Naqadi M, Erramli A, El-Metoui M, Al-Ahamdi M S G, Labadz A F, Bates C A and Ulrici W 1992 in preparation